Evolution of Nonlinear Alfvén Waves

in Streaming Inhomogeneous Plasmas

B. Buti[1,5]

Jet Propulsion Laboratory, California Institute of Technology, Pasadena, CA 91109

V.L. Galinski[2]

Scripps Institution of Oceanography, University of California, San Diego, LaJolla, CA 92093

V.I. Shevchenko[3]

Department of Electrical and Computer Engineering, University of California, San Diego, LaJolla, CA 92093

G.S. Lakhina[1] , B.T. Tsurutani[1], B.E. Goldstein[1]

and

P. Diamond and M.V. Medvedev[4]

Department of Physics, University of California, San Diego, LaJolla, CA 92093

[1]Jet Propulsion Laboratory, California Institute of Technology, Pasadena, CA 91109

[2]Scripps Institution of Oceanography, University of California, San Diego, LaJolla, CA 92093

[3]Department of Electrical and Computer Engineering, University of California, San Diego. LaJolla, CA 92093

[4]Department of Physics, University of California, San Diego, LaJolla, CA 92093

[5]E-mail: bbuti@jplsp.jpl.nasa.gov

ABSTRACT

Nonlinear evolution equation for Alfvén waves, propagating in streaming plasmas with nonuniform densities and inhomogeneous magnetic fields, is obtained by using the reductive perturbation technique. The governing equation is a modified derivative nonlinear Schrödinger (MDNLS) equation. Numerical solution of this equation shows that inhomogeneities exhibit their presence as an effective dissipation. The spatio-temporal evolution, of long wavelength Alfvénic fluctuations, shows that the wave steepens as it propagates. High frequency radiation is also observed in our simulations. Unlike coherent Alfvén waves in homogeneous plasmas, which can become non-coherent/chaotic only in the presence of a driver, MDNLS evolves into non-coherent/turbulent state without any driver, simply due to inhomogeneities. This clearly indicates that the integrability property of the DNLS, which allows coherent solitary solutions, is destroyed by inhomogeneities.

Subject headings: Turbulence, Solar Wind, Alfvén waves, Sun : Solar - terrestrial relations

1. Introduction

Large amplitude Alfvén waves have been observed in a variety of plasmas such as the solar wind, planetary bow shocks, interplanetary shocks, the solar corona, environment of comets etc. (Belcher and Davis 1971; Scarf et al. 1986). Alfvénic turbulence has been observed in the solar wind (Burlaga, 1983; Bavassano et al., 1982) as well as in the vicinity of comets (Tsurutani and Smith, 1986). Recently Marsch and Liu (1993) and Tu and Marsch (1995) have reported some observations of Alfvénic intermittent turbulence in the solar wind.

Implications of the existence of large-amplitude Alfvén waves in many cosmic plasmas have been investigated. Some of these examples include turbulent heating of the solar corona, coherent radio emissions, interstellar scintillations of radio sources, generation of stellar winds and extragalactic jets etc. Pettini et al. (1985) had carried out numerical simulations to look into the turbulent heating of the solar corona by these waves. Spangler (1991) had investigated Alfvénic turbulence in connection with interstellar scintillation of radio sources. Alfvén waves were shown to be the potential source for generation of stellar winds and extragalactic jets by Jatenco-Pereira (1995).

A number of MHD models have been suggested for the solar-wind turbulence (see recent review by Tu and Marsch, 1995 and references therein). Most of these models do not include dispersive effects and are restricted to homogeneous plasmas. A few of these models, which include inhomogeneities, are based on WKB theory. The latter however is incompatible for the studies of turbulence that involves a variety of different scales. Grappin and Velli (1996), in their expanding box model of the solar wind. however included non-WKB processes due to expansion. They showed the important role played by compressible effects in the evolution of solar wind turbulence.

To account for the dispersive nature of plasmas, one has to use Hall - MHD equations.

For finite but not very large amplitude Alfvén waves, the latter can be reduced to a single evolution equation, namely the DNLS equation (Kennel et al. 1988; Buti 1992, 1997). Hada et al. (1989) carried out an in-depth study of the DNLS equation and showed that the DNLS offers a variety of exact localized stationary solutions e.g., periodic envelope modulations; monochromatic waves; hyperbolic solitons; and algebraic solitons. However hyperbolic soliton solutions are found to be the most stable ones (Nocera and Buti, 1998). Ovenden et al. (1983) and Dawson and Fontán (1990) had proposed Alfvén soliton gas models for MHD turbulence in the solar wind. Dynamical evolution of nonlinear Alfvén waves, using the DNLS equation, has been studied by many investigators (Ghosh and Papadopoulos, 1987; Kennel et al. 1988; Buti 1992, 1997; Verheest and Buti, 1992). Ghosh and Papadopoulos (1987) and Hada et al. (1990) had included dissipative effects whereas kinetic effects were incorporated into the DNLS equation by Rogister (1971), Mjolhus and Wyller (1986, 1988) and Spangler (1989, 1990). Ghosh and Papadopoulos (1987) had studied the problem of generation of Alfvénic turbulence by numerically solving the driven dissipative DNLS by means of a spectral method. Hada et al. (1990) however, addressed the problem of Alfvénic chaos by studying the temporal evolution of the driven dissipative DNLS equation. They also included the discussion of slow, fast and intermediate shocks based on this equation. Following Hada et al. (1990), recently Chian et al. (1998), have suggested that Alfvénic intermittent turbulence, observed in the solar wind, could be generated by temporal chaos of driven Alfvén DNLS solitons. Medvedev et al. (1997) showed that inclusion of heat flux. modeled as ion-Landau damping, in the Kinetic Nonlinear Schrödinger (KNLS) equation (Medvedev and Diamond, 1996), leads to rotational discontinuities. All these investigations however, are restricted to homogeneous systems whereas most of the plasmas, where nonlinear Alfvén waves have been observed (Belcher and Davis 1971; Scarf et al. 1986), have inhomogeneous densities as well as magnetic fields.

By using the reductive perturbation method, Buti (1991) had rederived the governing

evolution equation for these waves in inhomogeneous plasmas. It was shown that the inhomogeneities lead to acceleration (deceleration) of solitary Alfvén waves depending upon the direction of propagation vis-a-vis density gradients. In this analysis, even though no explicit assumption about homogeneity of the magnetic field was made but because of the slab geometry used, implicitly the field considered was homogeneous.

In the present paper, we have removed this implicit restriction by incorporating spherical geometry. The evolution equation is rederived for inhomogeneous plasmas with arbitrary inhomogeneities. The evolution equation, in this case, turns out to be a modified DNLS (MDNLS) equation (see section. 2). Like DNLS equation, MDNLS is also not valid in regions with plasma $\beta \sim 1$ and magnetic field fluctuations $\delta B \sim B_0$. For solar wind closer to the sun where outward propagating Alfvén waves are generated, $\beta < 1$ and magnetic field fluctuations are not of the order of the ambient magnetic field. So, closer to the sun the MDNLS very well describes the evolution of finite-amplitude Alfvén waves. Numerical solution of the MDNLS equation, with solar wind parameters, exhibits features like wave steepening, emission of high frequency radiation, turbulent power spectra etc. The predicted power spectra are found to have spectral indices which increase with the heliocentric distances as observed in the solar wind turbulence (Belcher and Davis 1971; Bavassano et al. 1982). We also see a break-point in the frequency spectra. The break-point moves towards lower frequency with increasing heliocentric distance. In homogeneous plasmas, one can expect such an evolutionary behavior of Alfvén waves only when they are driven (Hada et al. 1990, Buti, 1992; Nocera and Buti, 1997; Buti and Nocera, 1999) or when they get coupled with the density fluctuations (Hada 1993; Buti et al. 1998). In the latter case nonlinear Alfvén waves are instead governed by a set of two nonlinear partial differential equations (Hada, 1993). Roychoudhury et al. (1997) studied the stability of this set of equations by means of Painléve analysis and showed that this coupled system is not an integrable system and thus no soliton solutions are possible. Buti et al. (1998) adapted

an alternative approach and studied evolution of the Alfvénic wave packets by means of Hall-MHD simulations. They found that the DNLS soliton is disrupted and evolves into a wave train. The disruption time is found to scale as B_s^{-4}, where B_s is the amplitude of the soliton (Velli et al., 1999).

The obvious conclusion one can draw, from the analysis presented here, is that inhomogeneities in density and magnetic field destroy the integrability properties of the DNLS equation that are solely responsible for coherent soliton solutions. Consequently coherent structures like solitons, which are exact solutions of the DNLS equation, evolve into noncoherent/turbulent structures characterized by power-law spectra.

2. EVOLUTION OF NONLINEAR ALFVÉN WAVES

The nonlinear equations governing Alfvén waves propagating in the radial direction are the two-fluid equations and the generalized Ohm's law (Kennel et al. 1988; Buti 1990, 1991):

$$\frac{\partial \rho}{\partial t} + \nabla \cdot (\rho \mathbf{v}) = 0, \tag{1a}$$

$$\rho \frac{d\mathbf{v}}{dt} = -\nabla p + \mathbf{J} \times \mathbf{B}, \tag{1b}$$

and

$$\frac{\partial \mathbf{B}}{\partial t} = \nabla \times \left[(\mathbf{v} \times \mathbf{B}) - \frac{1}{\rho}(\nabla \times \mathbf{B}) \times \mathbf{B} \right]. \tag{1c}$$

In eq.(1), $\mathbf{B}$ is normalized to $B_0(r = r_0)$, ρ to $\rho_0(r = r_0)$, $\mathbf{v}$ to $V_{A0} = B_0(r = r_0)/[4\pi\rho_0(r = r_0)]^{1/2}$, t to inverse of $\Omega_{i0} = \Omega_i(r = r_0)$, the ion cyclotron frequency and l to V_{A0}/Ω_{i0}; r_0 is simply some reference point.

We would like to point out here that the set of equations (1) would not be valid for systems with β (ratio of kinetic energy to magnetic energy) of order of unity because in that case kinetic effects become important. Moreover for $\beta \sim 1$, coupling between Alfvén waves and ion acoustic waves becomes significant (Hada, 1993). On using equations (1) in spherical co-ordinates and assuming no variations along θ and ϕ directions i.e., $\partial/\partial\theta = \partial/\partial\phi = 0$, eqs. (1) reduce to:

$$\frac{\partial\rho}{\partial t} + \frac{1}{r^2}\frac{\partial}{\partial r}(r^2\rho v_r) = 0, \tag{2a}$$

$$\rho\frac{dv_r}{dt} = -\frac{\partial p}{\partial r} - \frac{\partial}{\partial r}\frac{B_\perp^2}{2} - \frac{B_\perp^2}{2}, \tag{2b}$$

$$\rho\frac{d\mathbf{v}_\perp}{dt} = \frac{B_r}{r}\frac{\partial}{\partial r}(r\mathbf{B}_\perp), \tag{2c}$$

and

$$\frac{\partial\mathbf{B}_\perp}{\partial t} = \frac{1}{r}\frac{\partial}{\partial r}(B_r v_\perp - v_r B_\perp) + \frac{1}{r}\frac{\partial}{\partial r}\left[\frac{B\hat{\mathbf{e}}_r}{r\rho} \times \frac{\partial(\mathbf{B}_\perp r)}{\partial r}\right], \tag{2d}$$

where r is the radial distance, $\mathbf{B}_\perp = (B_\theta, B_\phi)$, $\mathbf{v}_\perp = (v_\theta, v_\phi)$, and $B_\perp^2 = (B_\theta^2 + B_\phi^2)$. For pressure, we use the adiabatic equation of state i.e., $p\rho^{-\gamma} = const$. In order to satisfy eq.(2a)

and the induction equation i.e., *div* $\mathbf{B}_0 = 0$, the equilibrium density $\rho_0(r)$ and the magnetic field $B_0(r)$ must satisfy the conditions:

$$B_0(r)\, r^2 \; = \; const \tag{3}$$

and

$$\rho_0(r)\, U(r)\, r^2 \; = \; const. \tag{4}$$

For weakly nonlinear systems, we can use reductive perturbation scheme to derive the evolution equation from Eqs.(2). Following the procedure outlined in Buti(1991), we use the following stretchings:

$$\eta = \epsilon^2 r; \qquad \xi = \epsilon \left[\int \frac{dr}{V(r)} - t \right]. \tag{5}$$

In Eq.(5) ϵ is the stretching parameter and $V(r)$ is the phase velocity of the Alfvén wave which is given by

$$V(r) = U(r) + \frac{B_0(r)}{\rho_0^{1/2}(r)}. \tag{6}$$

In Eq.(6), U is the equilibrium streaming plasma velocity.

On using the expansions for density, velocity, pressure and magnetic field appropriate to Alfvén Waves (cf. Buti 1991), for a spherically symmetric system, we obtain the following evolution (MDNLS) equation:

$$\frac{\partial B}{\partial \eta} + \frac{3\,U}{2\,V\,\eta}\,B + \frac{B}{4\,V\,(V-U)}\,\frac{\partial}{\partial \eta}\left(V^2 - U^2\right) \tag{7}$$
$$+\frac{(V-U)}{4\,B_0^2(\eta)\,V^2\,(1-\beta(\eta))}\,\frac{\partial}{\partial \xi}\left(B\,|\,B\,|^2\right) + \frac{i\,(V-U)^2}{2\,V^3\,B_0(\eta)}\,\frac{\partial^2\,B}{\partial \xi^2} = 0,$$

where $B = (B_\theta + i\,B_\phi)$, $\beta(\eta)$ is the plasma β, i.e., the ratio of kinetic pressure to magnetic pressure and $B_0(\eta)$ is the ambient magnetic field. In deriving Eq. (7), we have taken wave propagation as well as the ambient magnetic field along the radial direction and have neglected fifth order nonlinear terms. This equation, however, is valid for arbitrary inhomogeneities. We may note that for nonstreaming uniform plasmas i.e., for $U = 0$ and $\rho_0(r) = 1$, $V \to 1$ and Eq. (7) reduces to the well known DNLS equation (Kennel et al. 1988), which gives an exact soliton solution. It is interesting to observe that this modified DNLS (Eq (7)), besides having additional two linear terms in B, has variable co-efficients for nonlinear and dispersive terms. Because of these complicated variable co-efficients, it is not possible to find an analytical solution to Eq. (7) and one has to look for its numerical solution. We have done this on the assumption that solving a single nonlinear partial differential equation (pde) is much simpler than handling a set of pdes, e.g., Hall MHD equations, that requires a simulation code with expanding box. We are now persuing the latter course and hope to be reporting these results in the near future.

3. NUMERICAL COMPUTATIONS

For numerical solution of eq.(7), we use the spectral collocation method. We rewrite this equation as,

$$\frac{\partial B}{\partial \eta} + f(\eta)B + \alpha_1(\eta)\frac{\partial}{\partial \xi}(|B|^2 B) + i\alpha_2(\eta)\frac{\partial^2 B}{\partial \xi^2} = 0. \tag{8}$$

Since eq. (8) has temporal and spatial variables interchanged, we write the approximate solution for B as a Fourier expansion in time instead of space, namely

$$B(\xi, \eta) = \sum_{k=-N}^{N-1} b_k(\eta)e^{-i\lambda_k \xi}. \tag{9}$$

Note that B is assumed to be periodic in time, with period T and frequency $\lambda_k = 2\pi k/T$.

The spectral collocation (or pseudospectral) method requires introduction of collocation points (grid points) ξ_i. For evaluation of the cubic nonlinear term of eq.(8), we use the padding method (alternatively known as 3/2 rule) for dealiasing (Conuto et al. 1988). According to this scheme, the Fourier transform for the nonlinear term can be represented by,

$$|B(\xi_i, \eta)|^2 B(\xi_i, \eta) = \sum_{k=-M}^{M-1} g_k(\eta)e^{-i\lambda_k \xi_i}. \tag{10}$$

In order to be sure that aliasing errors are not introduced by this form of approximate solution, summation index M must be greater than $3N/2$; N is the summation index used in Eq.(9). This simply means that nonlinear term is calculated by using larger number of grid points compared to the number used in the original expansion for B in Eq. (9). Thus in Eq.(9), $b_k = 0$ for $N < |k| < M$ i.e., high frequency harmonics of b_k (for $|k| > N$ only) are neglected. This effectively means introduction of some artificial dissipation in the system.

The standard Galerkin version of the weighted residual method is used for discretisation, with exponential weighting functions $W_k(\xi) = \exp(-i\lambda_k \xi)$. In other words semidiscrete system of equations is obtained by using the relation

$$\int_0^T R(\xi, \eta) W_k^\star(\xi) d\xi = 0, \qquad k = -N, \ldots, N-1, \tag{11}$$

where $R(\xi, \eta)$ is the residual of the DNLS equation, namely

$$R(\xi, \eta) = \sum_{n=-N}^{N-1} \left[\frac{\partial b_n}{\partial \eta} + f(\eta)b_n - i\alpha_1 \lambda_n g_n(\eta) - i\alpha_2 \lambda_n^2 b_n \right] W_n(\xi). \tag{12}$$

Taking this weighted residual integration, we obtain the system of ordinary differential equations for the coefficients $b_k(\eta)$, which can be solved using either the second order Adams-Bashforth predictor – Adams-Moulton corrector pair, or the adaptive step size iterative scheme with accuracy check. The accuracy check in the second method assures that small scale structures appearing in the solution have physical origin, rather than being numerical artifacts.

We do not need to introduce any artificial dissipation for the numerical solution of MDNLS. In our case, inhomogeneous terms formally play the role of effective dissipation. Moreover, the iterative scheme of dealiasing, that we have used for calculation of nonlinearity, keeps the soliton solution of the conservative homogeneous DNLS unchanged for much longer distances than reported here. This could alternatively be achieved even without dealiasing, but with a fine enough grid.

As mentioned earlier, the problem of wave propagation is solved as an evolutionary problem in space. For this purpose, we assume that there is an influx of waves at one end of the interval (e.g., closer to the Sun in case of solar wind plasma) and the waves are propagating outward from the Sun. The influx is assumed periodic in time.

For numerical solution, we have considered two cases. 1) Evolution of an initial Alfvén soliton which is an exact solution of DNLS equation and 2) evolution of an amplitude-modulated circularly polarized wave. The reason for picking up the DNLS soliton solution as the initial condition is the following: Locally in the regions closer to the sun, where

Alfvén waves are generated, DNLS is a good representation of Alfvén waves. Moreover one of the basic properties of any evolution equation, e.g., DNLS equation, which can be solved exactly by means of the Inverse Scattering Transform method (Kaup and Newell, 1978), is to transform any localized initial condition to a soliton solution. Dawson and Fontan (1988) numerically solved the DNLS equation with an initial modulated Gaussian packet and confirmed its decay into soliton solution. For the soliton case we take,

$$B(\xi, r_0) = \frac{B_{max}\, e^{i\theta\,(\xi)}}{cosh^{1/2}\,\psi}, \tag{13}$$

with

$$\psi = (\xi - L/2)\, B_{max}^2\, /(\, 2\,\delta), \tag{14}$$

$$\theta(\xi) = \frac{3}{2}\, tan^{-1}\, (sinh\,\psi) \tag{15}$$

and

$$\delta = \frac{2}{V}\, (1 - \beta)\, (V - U). \tag{16}$$

B_{max} in Eq.(13) is the amplitude of the initial soliton normalized to $B_0\,(r_0)$ and L is the domain length. We would like to point out that the solution given in Eq.(13) is different than the one we had used earlier (Verheest and Buti 1992; Nocera and Buti 1996; Buti et al. 1998). In the soliton solution (Mjolhus 1978), there are two arbitrary constants κ_0 and ν_0. Earlier we had taken $\nu_0 = 0$ and now for Eq.(13) κ_0 has been taken to be zero.

For Fig.1 we have taken the reference point, $r_0 \equiv R_s$ (R_s being the solar radius). The other simulation parameters chosen are : $\beta\,(R_s) = 0.01.$ and $r_0\,\Omega_{i0}\,/\,V_{A0} = 10^6$ at $r_0 =$

R_s. Fig.1 shows the variation of $B_{max}(r)$ / B_0 (r) with heliocentric distance for different initial conditions. In all the three cases, we see that magnetic field fluctuations increase with increasing r. This is in agreement with the observations (Klinglesmith 1997). It is interesting to note that despite B_{max} decreasing with increasing heliocentric distance (see Fig.2), the ratio $B_{max}(r)$ / B_0 (r) goes up. So an obvious conclusion one can draw is that $B_0(r)$ decreases much faster compared to $B_{max}(r)$.

EDITOR: PLACE FIGURE ?? HERE.

Fig.1

Fig.2 (corresponding to reference point $r_0 = R_0 = 0.1AU$) shows time evolution of the field starting with soliton amplitude $B_{max} = 0.036$ $B_0(R_0)$, $U_0 = 1.5$ V_{A0} and β $(R_0) = 0.05$. We find that amplitude of the soliton goes down as the wave propagates away from the sun. This shows that inhomogeneities in density and magnetic field are providing the source for physical dissipation. Similar dissipative effects of inhomogeneities, in connection with modulated ion-acoustic waves, were reported by Mohan and Buti (1979). We also see the steepening of the wave and the high-frequency radiation on the leading edges. The high-frequency radiation has frequencies larger than the Alfvén frequency but much smaller than whistler frequencies. Steepening is found to increase with increasing heliospheric distances. The corresponding spectra for the field fluctuations are shown

EDITOR: PLACE FIGURE ?? HERE.

Fig.2

in Fig.3. Note the break in the power spectra; the break-point moves towards lower frequencies with an increase in the heliocentric distance. This trend is similar to the one

shown by Helios observations (Bavassano et al.1982). Moreover, we find that the spectral index (α) increases from 1.6 to 2.6 with an increase in the radial distance from $0.5 - 0.9AU$. The observed values of α, according to Mariner 5 (Belcher and Davis 1971) and Helios 1 and 2 (Bavassano et al. 1982) data range between 1.2 - 2.2.

EDITOR: PLACE FIGURE ?? HERE.

Fig.3

EDITOR: PLACE FIGURE ?? HERE.

Fig.4

Ideally one would like to see the evolution of Alfvén waves starting from the photosphere all the way to 1AU but to achieve this one faces some practical difficulties. If one uses one single scale for the numerical solution of the MDNLS in the range $1R_s < r < 1AU$, the computer time is formidably large. For this reason, we solved the MDNLS by using two different scalings - one closer to the sun and the other one for regions closer to 1AU, by taking appropriate solar-wind parameters for the two regions. The qualitative behavior in the two regions was found similar. Observations are available only for $r > 0.3AU$; so, we are not reporting the numerical results obtained for the region near the photosphere. The difference in the observed values of α and the ones shown in Fig.3, could be because we have taken the ambient magnetic field B_0 as a function of r only i.e., $B_0 = B_0(r)$. Closer to 1AU, this is not a very good approximation. In future we would consider a more general case of $B_0 = B_0(r, \theta)$ by incorporating cylindrical symmetry. To determine the cause of this difference, we would also incorporate kinetic effects in our model.

For the second case, we consider an amplitude-modulated circularly polarized wave. The reason for picking up an amplitude-modulated wave rather than a purely circularly

polarized wave is simply because the latter is an exact solution of DNLS and it does not undergo any nonlinear evolution.The modulated initial wave profile, in this case, can be represented by two initially excited harmonics in the expansion for B of Eq.(9). For left hand circularly polarized (LHP) wave, we take these two harmonics as $k = -1$ and -2 (Medvedev et al. 1997). Thus in accordance with Eq.(9), for LHP wave, we take

$$B(R_0,\ t)\ =\ 0.01\ [\exp\frac{2\ i\ \pi\ t}{T_{max}}\ +\exp\frac{4\ i\ \pi\ t}{T_{max}}],\tag{17}$$

with $T_{max} = 19200\ \pi\ \Omega_{i0}^{-1}$. The evolution of Alfvén waves in this case is shown in Fig.4. The evolution in this case is much slower compared to the soliton case. High frequency radiation is seen only for $r\ >\ 0.9$ AU. The spectra (not shown) also do not evolve into power spectra during the periods considered here.

4. CONCLUSIONS

Large amplitude Alfvén waves propagating radially in plasmas, with inhomogeneous densities and magnetic fields, are governed by the MDNLS equation. Numerical solution of this equation, for the case of solar wind, shows that the Alfvén soliton evolves with space and time and shows features e.g., evolution of magnetic field fluctuations, power spectra, wave steepening and emission of high-frquency radiations. We observe a cut-off in the power spectra; the cut-off is found to move towards lower frequencies with increasing heliocentric distance. Moreover the spectral index α goes up with the helicentric distance. The spectral indices of the predicted power spectra from our model range between 1.6 - 2.6 wheras for the same frequency range the observed spectral indices from Mariner 5 (Belcher and Davis 1971) and Helios 1 and 2 (Bavassano et al. 1982) data range between 1.2 - 2.2. In order to look for better quantitative agreement of α with the observed spectral indices, we plan

to use cylindrical geometry which is a better approximation closer to 1AU. To overcome the shortcomings of DNLS/MDNLS model used in the present investigation, we would also include kinetic effects as well as coupling of magnetic field and density fluctuations. For our numerical solutions herein, we have used the solar wind parameters but the model is very general and can be applied to other cosmic plasmas also. We also plan to extend this model to driven dissipative Alfvénic systems to investigate the problem of intermittent turbulence. These results will be reported in a forthcoming paper.

We emphasize that even though we initially start with a coherent structure like the DNLS soliton, because of inhomogeneities embedded in our MDNLS equation, it evolves into a non-coherent/turbulent (not fully developed) state. This could be a good reason for the non-existence of Alfvén solitons in the solar wind. The complete integrability property of the DNLS is clearly destroyed by these inhomogeneities. Following the mathematical analysis of Roychoudhury et al. (1997), we plan to do the Painléve analysis of the MDNLS equation to determine its stability properties.

REFERENCES

Bavassano, B., Dobrowolny, M., Mariani, F., & Ness, N. F. 1982, *J. Geophys. Res., 87*, 3617

Belcher, J. W., & Davis, L. 1971 , *J. Geophys. Res., 76*, 3534

Burlaga, L. F. 1983, *Rev. Geophys. Space Phys. 21*, 363

Buti, B. 1990, in *Solar and Planetary Plasma Physics, Ed. B. Buti* (World Scientific, Singapore), 92

Buti, B. 1991, *Geophys. Res. Lett., 18*, 809

Buti, B., 1992 *Jou. Geophys. Res., 97* , 4229

Buti, B., Jayanti, V., Viñas, A. F., Ghosh, S., Goldstein, M. L., Roberts, D. A., Lakhina, G. S., & Tsurutani, B. T. 1998, *Geophys. Res. Letts.*, 25, 2377

Buti, B., & Nocera, L. 1999, in *Solar Wind Nine, Eds. Shadia Habbal et al.*, American Inst. Phys. (in press)

Canuto, C., Hussaini, M.Y., Quarteroni, A., & Zang, T.A. 1987 *Spectral Methods in Fluid Dynamics* (Springer Verlag, New York), 84

Chian, A. C.-L., Borotto, F.A., & Gonzalez, W.D. 1998, *Astrophys.J., 505*, 993

Dawson, S.P., & Fontán, C.F. 1988, *Phys. Fluids, 31*, 83

Dawson, S.P., & Fontán, C.F. 1990, *Astrophys.J., 348*,761

Ghosh, S., & Papadopoulos, K. 1987, *Phys. Fluids, 30*, 1371

Grappin, R., & Velli, M. 1996, *J. Geophys. Res.,101*, 425

Hada, T., Kennel, C. F., Buti, B. 1989, *Jou. Geophys. Res.,94*, 65

Hada, T., Kennel, C. F., Buti, B., & Mjolhus, E. 1990, *Phys. Fluids, B2*, 2581

Hada, T. 1993, *Geophys. Res. Letts., 20*, 2415

Jatenco-Pereira, V. 1995, *Physica Scripta, T60*,113

Kaup, D.J., & Newell, A.C. 1978, *J. Math. Phys., 19,* 798

Kennel, C. F., Buti, B., Hada, T., & Pellat, R. 1988, *Phys. Fluids, 31,* 1949

Klinglesmith, M. 1997 , in *The Polar Solar Wind from 2.5 to 40 Solar Radii: Results of Intensity Scintillation Measurements (Ph.D. Dissertation), UCSD*

Marsch, E. & Liu, S. 1993, *Ann. Geophys.,11,* 227

Marsch, E. & Tu, C.Y. 1996, *J. Geophys. Res.,101,* 11149

Medvedev, M. V., & Diamond, P. H. 1996, *Phys. Plasmas, 3,* 863

Medvedev, M. V., Shevchenko, V. I., Diamond, P. H., & Galinsky, V. L. 1997,*Phys. Plasmas, 4,* 1257

Mjolhus, E. 1978, *J. Plasma Phys.,19,* 437

Mjolhus, E., & Wyller, J. 1986, *Physica Scripta, 33,* 442

Mjolhus, E., & Wyller, J. 1988 , *J. Plasma Phys., 40,* 299

Mohan, M., & Buti, B. 1979, *Plasma Phys., 21,* 713

Nocera, L., & Buti, B. 1996, *Physica Scripta, T63,* 186

Nocera, N., & Buti, B. 1997 , in *New Perspectives in the Physics of Mesoscopic Systems, ed. S. De Martino et al., World Scientific, Singapore,* 225

Nocera, L., & Buti, B. 1998, *Cont. Fusion and Plasma Phys.,22C,* 2295

Ovenden, C.R., Shah, H.A., & Schwartz, S.J. 1983, *J. Geophys. Res., 88,* 6095

Pettini, M., Nocera, L., & Vulpiani, A. 1985 in *Chaos in Astrophysics, ed. J.R. Buchler et al., Dordrecht: Reidel,* 305

Rogister, A. 1971, *Phys. Fluids 14,* 2733

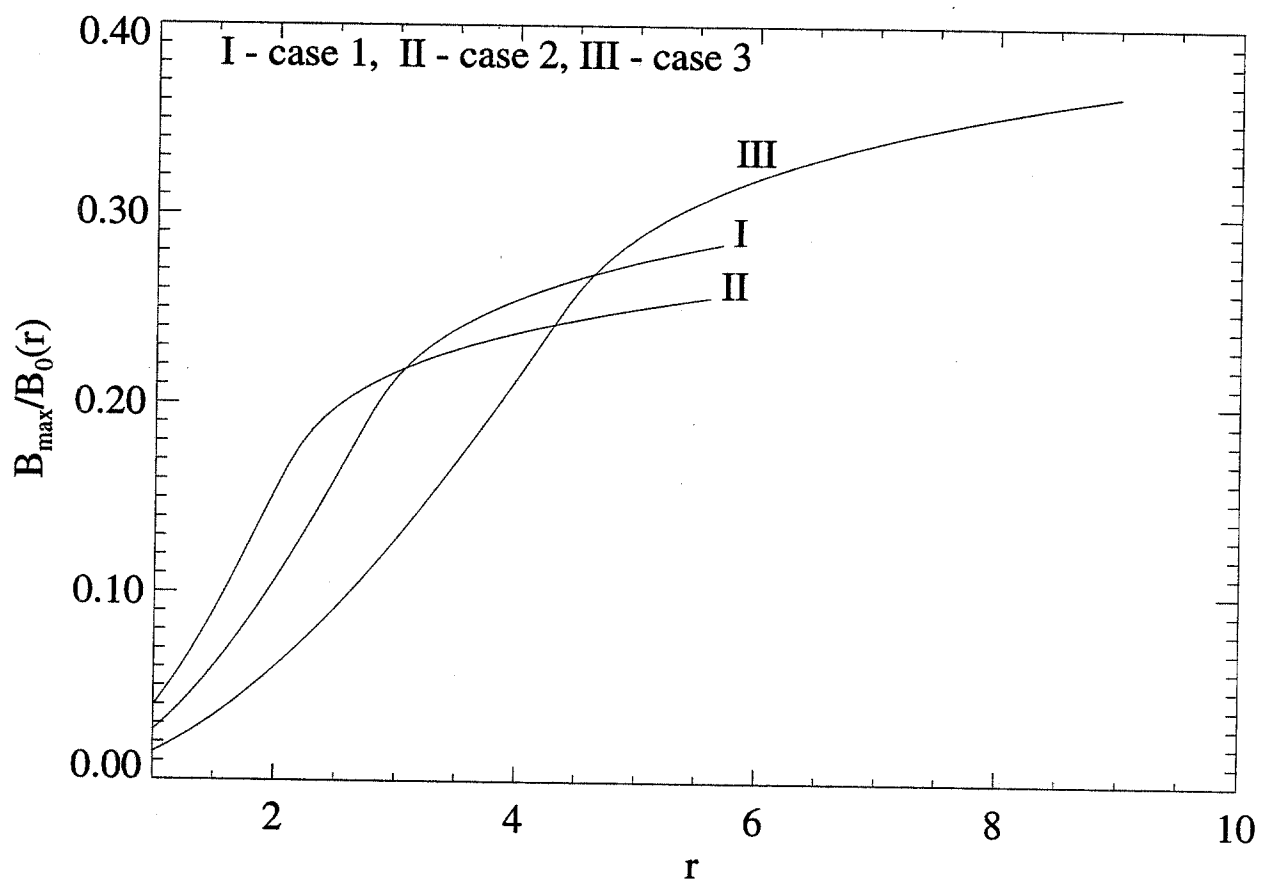Roychoudhury, A., Buti, B., & Dasgupta, B. 1997, *Australian J. Phys.,51,* 125

Scarf, F. L., Coroniti, F. V., Kennel, C. F., Gurnett, D. A., & Smith, E. J. 1986, *Science,* *232*, 382

Spangler, S. R. 1989, *Phys. Fluids, B1*, 1738

Spangler, S. R. 1990, *Phys. Fluids, B2*, 407, 1990

Spangler, S. R. 1991, *Astrophys.J., 376*, 540

Tsurutani, B. T., & Smith, E. J. 1986, *Geophys. Res. Lett.13*, 259

Tu, C.Y., & Marsch, E. 1995, *Space Sci. Rev., 73*, 1

Velli, M., Buti, B., Goldstein, B.E., & Grappin, R. 1999, in *Solar Wind Nine, Eds. Shadia Habbal et al.*, American Inst. Phys. (in press)
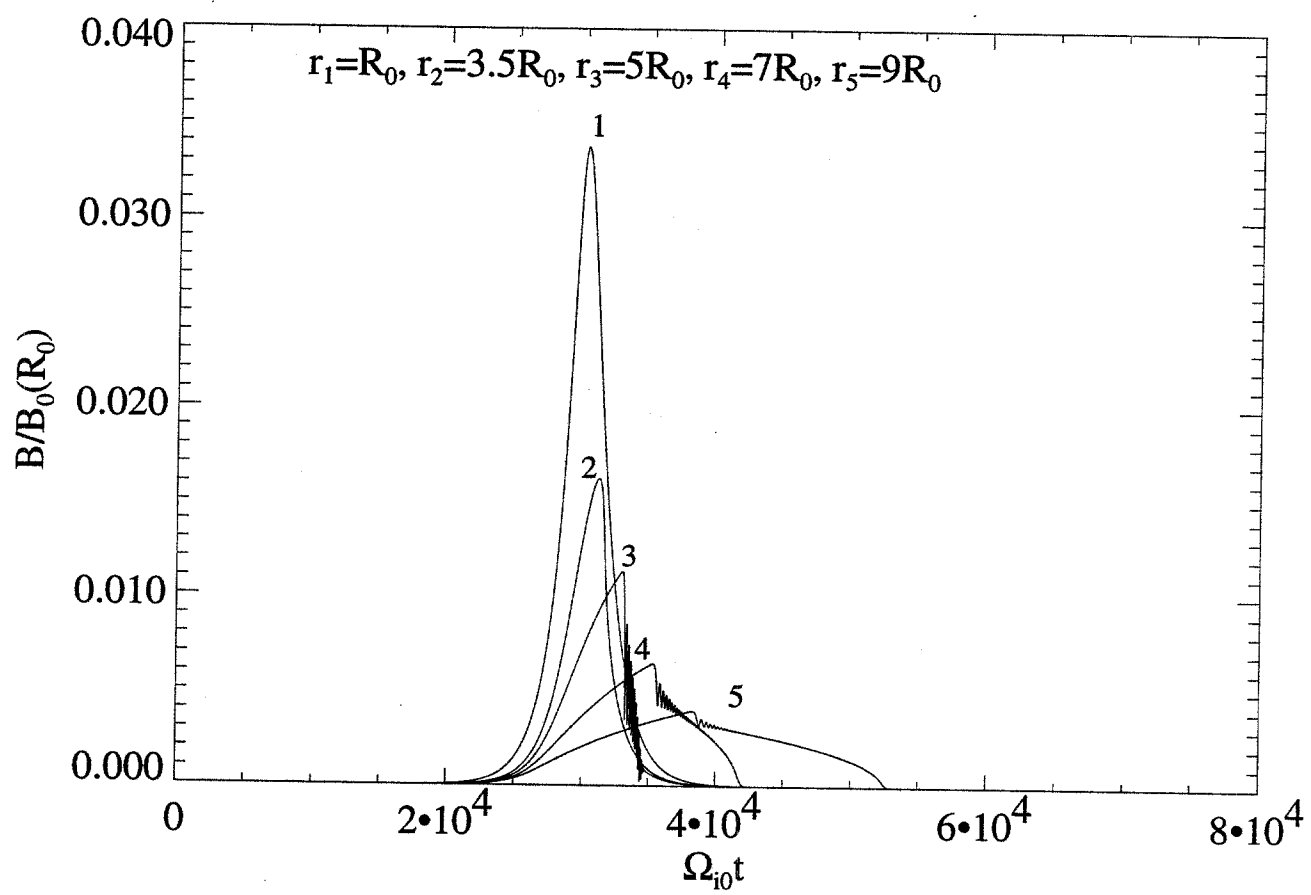
Verheest, F., & Buti, B. 1992, *J. Plasma Phys., 47*, 15

Fig. 1.— shows variation of $B_{max}(r)$ / B_0 (r) with heliocentric distance r / R_s for 3 cases with β (r_0) = 0.01. and r_0 Ω_{i0} / V_{A0} = 10^6. For case 1, B_{max} = 0.026 B_0 (r_0) and T_{max} = 64000 π Ω_{i0}^{-1}; case 2, B_{max} = 0.039 B_0 (r_0) and T_{max} = 64000 π Ω_{i0}^{-1} and case 3, B_{max} = 0.014 B_0 (r_0) and T_{max} = 192000 π Ω_{i0}^{-1}.
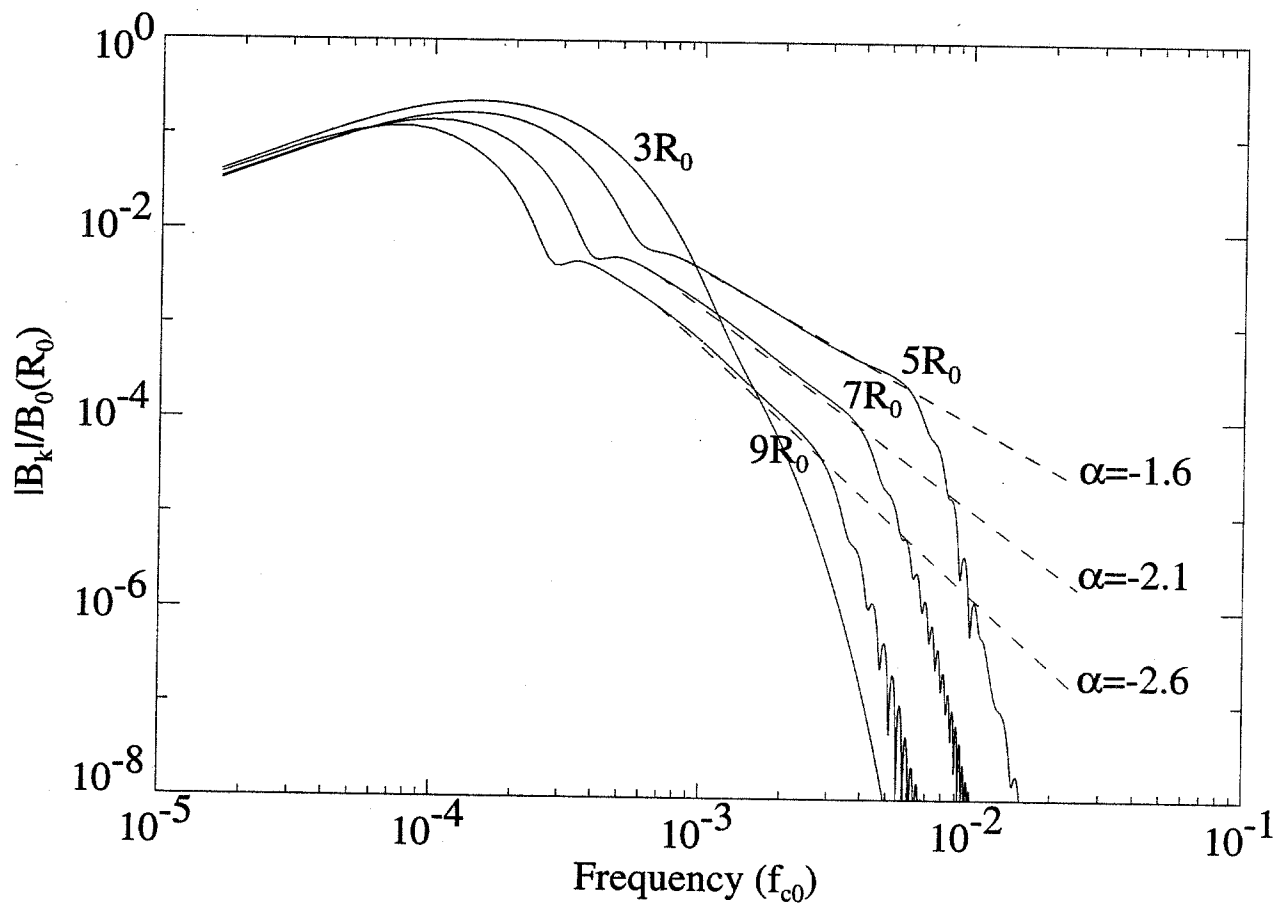
Fig. 2.— shows evolution of B / B_0 (r_0) with t for B_{max} (R_0) = 0.036, R_0 = 0.1 AU. U_0 = 1.5 V_{A0} and β (R_0) = 0.05. Curves labelled 1, 2, 3, 4 and 5 correspond to r = 0.1 AU. 0.35 AU, 0.5 AU, 0.7 AU and 0.9 AU. .

Fig. 3.— shows power spectra for heliospheric distances 0.3 AU, 0.5 AU, 0.7 AU and 0.9 AU. The parameters used are same as for Fig.2.

Fig. 4.— shows the evolution of B / B_0 (R_0) with t for initially circularly polarized wave for heliospheric distances 0.1 AU, 0.7 AU, 0.9 AU and 1.05 AU. The parameters used are same as for Fig.2.
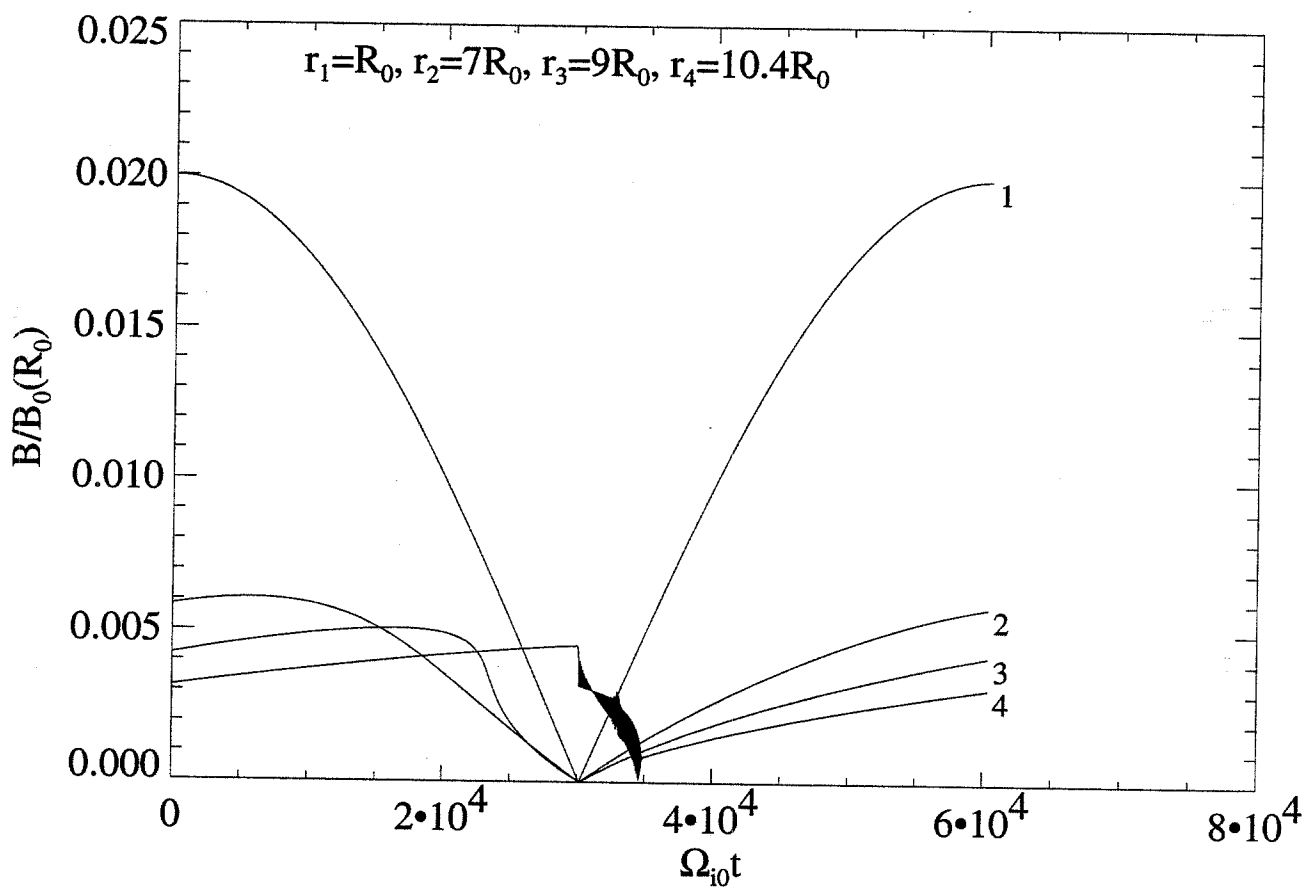
I - case 1, II - case 2, III - case 3

$\frac{B_{max}}{B_0(r)}$

Fig 1

Fig 2

Fig 3

$r_1=R_0$, $r_2=7R_0$, $r_3=9R_0$, $r_4=10.4R_0$

Fig. 4